PROCEEDINGS OF SCIENCE

An improvement of glueball mass calculations using gradient flow

Keita Sakai* **and Shoichi Sasaki**

Department of Physics, Tohoku University, Sendai 980-8578, Japan

E-mail: sakai@nucl.phys.tohoku.ac.jp, ssasaki@nucl.phys.tohoku.ac.jp

Removing ultraviolet noise from the gauge fields is necessary for glueball spectroscopy in lattice QCD. It is known that the Yang-Mills gradient flow method is an alternative approach instead of link smearing or link fuzzing in various aspects. In this work we study the application of the gradient flow technique to the construction of the extended glueball operators. We examine a simple application of the gradient flow method, which has some problems in glueball mass calculations at large flow time because of its nature of diffusion in space-time. To avoid this problem, the spatial links are evolved by the "spatial gradient flow", that is defined to restrict the diffusion to spatial directions only. We test the spatial gradient flow in calculations of glueball two-point functions as a new smearing method, and then discuss its efficiency in comparison with the original gradient flow method and traditional smearing methods.

The 38th International Symposium on Lattice Field Theory, LATTICE2021 26th-30th July, 2021
Zoom/Gather@Massachusetts Institute of Technology

*Speaker

PoS(LATTICE2021)333

1. Introduction

The existence of composite states consisting solely of gluons, called glueballs, is one of the important predictions of QCD. Since none of them have been identified in experiments as a glueball state, the lattice QCD results play an essential role in studying properties of the glueball states including their masses. However, ultraviolet noise from the gauge fields makes it difficult to calculate the glueball spectrum in lattice QCD. Therefore, the noise reduction technique such as the link smearing or fuzzing procedure plays an increasingly important role on the construction of the extended glueball operators. Several smearing techniques are developed for this purpose, such as APE smearing [1], or stout smearing [2]. Recently, it is known that the Yang-Mills gradient flow method [3] is an alternative approach instead of the link smearing or the link fuzzing in various aspects. Indeed, the gradient flow equation can be regarded as a continuous version of the link fuzzing step in the stout smearing with the small smearing parameter at the finer lattice spacing [3, 4]. Therefore, in this study, we investigate the application of the gradient flow technique to the glueball calculation and also demonstrate its effectiveness in comparison to the conventional method.

2. Smearing methods

2.1 Original gradient flow

The Yang-Mills gradient flow on the lattice is a kind of diffusion equation where the link variables $U(x,\mu)$ evolve smoothly as a function of fictitious time τ (denoted as flow time). The associated flow $V_\tau(x,\mu)$ of the link variables (hereafter called as the Wilson flow) is defined by the following equation with the initial conditions $V_\tau(x,\mu)|_{\tau=0} = U(x,\mu)$:

$$\frac{\partial}{\partial\tau}V_\tau(x,\mu) = -g_0^2\partial_{x,\mu}S_W(V_\tau(x,\mu))V_\tau(x,\mu) \tag{1}$$

where g_0 is the bare coupling, S_W denotes the standard Wilson plaquette action in terms of the flowed link variables. According to Eq. (1), the link variables are diffused in the four-dimensional *space-time*, so that the Wilson flow is approximately spread out in a Gaussian distribution with the diffusion radius (or length) of $R_d = \sqrt{8\tau}$ [3]. Although such smearing procedure works well with the longer flow time, too much smearing will destroy or hide the true temporal correlation of the glueball two-point function due to the overlap of two glueball operators given by the Wilson flow. Therefore, the longer flow is not applicable for the glueball spectroscopy to avoid *over smearing* [5].

2.2 Spatial gradient flow as a new smearing method

As described in Sec 2.1, the previous attempt to apply the gradient flow to the glueball spectroscopy is not fully satisfactory. We propose the "spatial gradient flow" as a new smearing method in order to overcome the limited usage of the Wilson flow due to over smearing. The spatial gradient flow is defined to restrict the diffusion to spatial directions only, so that the spatial links $U(x,i)$ are evolved into the spatial Wilson flow $\mathcal{V}_\tau(x,i)$ as the initial conditions of $\mathcal{V}_\tau(x,i)|_{\tau=0} = U(x,i)$ in the following gradient flow equation:

$$\frac{\partial}{\partial\tau}\mathcal{V}_\tau(x,i) = -g_0^2\partial_{x,i}S_{\text{splaq}}(\mathcal{V}_\tau(x,i))\mathcal{V}_i(x,i) \tag{2}$$

where $S_{\rm splaq}$ denotes the spatial plaquette term in the Wilson plaquette action

$$S_{\rm splaq} = \frac{2}{g_0^2} \sum_{x,i>j} \mathrm{Tr}\left\{1 - \mathrm{Re}\left[\mathcal{V}_\tau(x,i)\mathcal{V}_\tau(x+i,j)\mathcal{V}_\tau^\dagger(x+j,i)\mathcal{V}_\tau^\dagger(x,j)\right]\right\}. \tag{3}$$

The indices i and j run only over spatial directions. Since the spatial Wilson flow is diffused only *in three-dimensional space*, its diffusion radius is given by $\mathcal{R}_d = \sqrt{6\tau}$. We will later show that this new smearing works well even for the glueball spectroscopy without over smearing.

3. Numerical results

3.1 Simulation details

We perform the pure Yang-Mills lattice simulations using the Wilson plaquette action with a fixed physical volume ($La \approx 1.6$ fm) at four different gauge couplings ($\beta = 6/g_0^2 = 6.2$, 6.4, 6.71 and 6.93). All lattice spacings are set by the Sommer scale ($r_0 = 0.5$ fm) [6, 7]. For both original and spatial gradient flows, the forth-order Runge-Kutta scheme is used with an integration step size of $\epsilon = 0.025$. The flow time τ is given by $n_{\rm flow} \times \epsilon$ where $n_{\rm flow}$ denotes the number of flow iterations.

Table 1: Summary of simulation parameters: gauge coupling, lattice size ($L^3 \times T$), lattice spacing (a), spatial physical size (La), the Sommer scale (r_0), the number of the accumulated gauge configurations ($N_{\rm conf}$), the number of measurements per configuration ($N_{\rm meas}$) and the number of total measurements ($N_{\rm total} = N_{\rm conf} \times N_{\rm meas}$). All lattice spacings are set by the Sommer scale ($r_0 = 0.5$ fm) [6, 7].

$\beta = 6/g_0^2$	$L^3 \times T$	a [fm]	La [fm]	r_0/a (Ref. [7])	$N_{\rm conf}$	$N_{\rm meas}$	$N_{\rm total}$
6.2	$24^3 \times 24$	0.0677	1.63	7.38	4000	4	16000
6.4	$32^3 \times 24$	0.0513	1.64	9.74	3000	1	3000
6.71	$48^3 \times 48$	0.0345	1.66	14.49	500	4	2000
6.93	$64^3 \times 64$	0.0256	1.64	19.48	300	4	1200

3.2 Results obtained from the gradient flows

We first recapitulate the problem of a simple application of the original gradient flow to calculate the glueball two-point functions. In this subsection, we focus on the results of the 0^{++} glueball mass spectrum calculated on a 32^4 lattice at $\beta = 6.4$ with a simple plaquette for glueball operator as a typical example. In Fig. 1, we show the results of two-point functions (left panel) and their effective mass plots (right panel) using the original gradient flow with three values of flow time τ, which are represented by the values of the diffusion radius $R_d = \sqrt{8\tau}$ in lattice units.

As shown in the left panel of Fig. 1, the statistical errors on the glueball two-point function are dramatically reduced up to the large time slice region as the flow time increases. However, the temporal correlation in the region of $t < R_d$ become suffered from the overlap of two glueball operators which are smeared in space-time according to a Gaussian spread. In fact that if the two-point function $C(t)$ forms a Gaussian shape, $C(t) \propto C_{\rm guass}(t) = e^{-t^2/(2\sigma_t^2)}$ with a Gaussian width

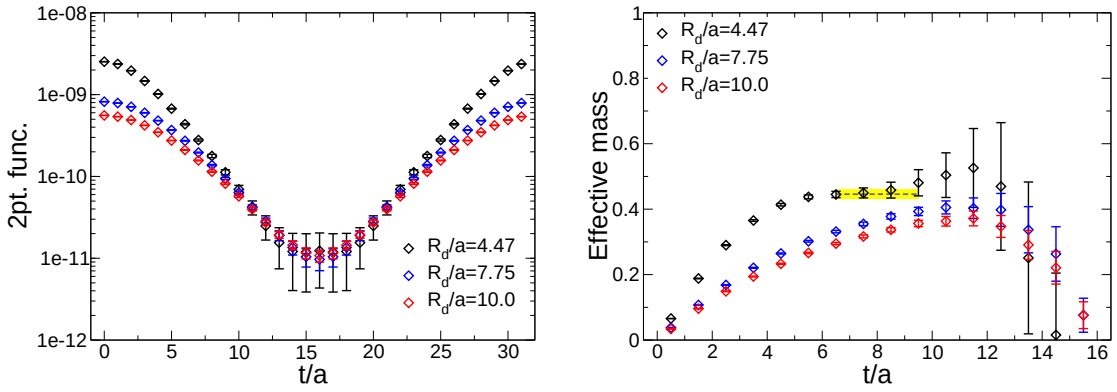

Figure 1: Examples of the 0^{++} glueball results obtained from **the original gradient flow**: two-point functions (left) and their effective mass plots (right) as functions of the time slice t for three values of flow time τ.

σ_t associated with the diffusion radius R_d like $\sigma_t \propto R_d$, its effective mass gives rise to a peculiar t-dependence as below.

$$m_{\text{eff}} = -\frac{d}{dt}\log C(t) \to \frac{t}{\sigma_t^2} \propto \frac{t}{R_d^2}, \tag{4}$$

whose value linearly increases from zero with a coefficient of $1/\sigma_t^2$ as a function of the time slice t. This feature can be observed in the right panel of Fig. 1, where each effective mass approximately starts from zero and linearly raise up to around $t \approx R_d$ with increasing of the time slice t. Furthermore, as expected in Eq. (4), it is easily observed that the slope of the linear dependence decreases with the larger flow time. When the shorter flow time such as the case of $R_d/a = 4.47$ is chosen to avoid over smearing, the effective mass shows a plateau behavior in the region of $t > R_d$. However, the effective mass tends to approach zero toward the temporal midpoint ($t/a = 16$) due to the wrap-around effect, so that the plateau region highly depends on the choice of the flow time. As a result, the plateau behavior is too uncertain to extract the ground-state mass of the glueball with high accuracy.

We next show the results obtained from the spatial gradient flow in Fig. 2. First of all, in the left panel of Fig. 2, the exponential fall-offs are clearly seen for all three values of the flow time and their slopes in the asymptotic region are independent of the choice of the flow time. The latter point can be confirmed in the right panel of Fig. 2, where their effective mass plots are displayed. For sufficiently large flow time ($\mathcal{R}_d/a > 6.71$), the plateau behavior in the effective mass plot does not change with variation in flow time. This is a great advantage compared to the original gradient flow. Furthermore, the plateau behavior starts at a smaller time slice, where the true temporal correlation of the glueball two-point function is kept unaffected during the smearing procedure contrast to the original gradient flow. It is another advantage for extracting the ground-state mass of the glueball with high accuracy, though the large statistical fluctuations still remain in the large t region.

Finally, we calculate the ground-state mass of the 0^{++} glueball by fitting the glueball two-point function with a single exponential form for both gradient flow cases. The choice of $R_d/a = 4.47$ for the original gradient flow is taken to avoid over smearing, while the data with $\mathcal{R}_d/a = 8.66$ is

used for the spatial gradient flow as a typical example. The 0^{++} glueball masses are respectively evaluated from two types of the gradient flow as below:

$$aM_{0^{++}} = \begin{cases} 0.446(14) & \text{(original gradient flow)} \\ 0.402(9) & \text{(spatial gradient flow)} \end{cases} \tag{5}$$

Each of the central values and errors is displayed as a blue dotted line and yellow shaded bands within the fit range in the right panel of Fig. 1 and Fig. 2 . The statistical error on the original gradient flow result is slightly larger than that of the spatial gradient flow, while the central value of the former is slightly overestimated in comparison to the latter. Recall that the central value of the original gradient flow result tends to be lower when the flow time is taken longer regardless of over smearing. Needless to say, the original gradient flow requires the optimal choice of the flow time, while the spatial gradient flow result becomes stable for the large flow time.

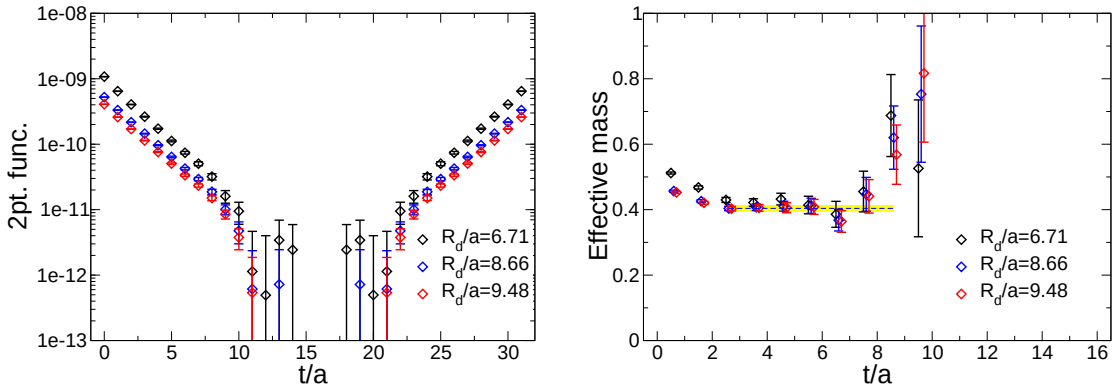

Figure 2: Examples of the 0^{++} glueball results obtained from **the spatial gradient flow**: two-point functions (left) and their effective mass plots (right) as functions of the time slice t for three values of flow time τ.

3.3 Spatial gradient flow vs. Stout smearing

We will later show numerical equivalence between the spatial gradient flow and the stout smearing in the glueball calculations. As emphasized in Ref. [2], the stout smearing is a relatively new type of smearing technique, which can keep the differentiability with respect to the link variables during the smearing procedure. This property is maintained by the use of the exponential function in the link fuzzing algorithm to remain within the SU(3) group. For the gradient flow, the numerical integrations of Eqs. (1) and (2) with respect to the flow time are perform with the Runge-Kutta scheme to obtain the Wilson flow as a solution of Eqs. (1) and (2). This procedure requires the exponentiation of the "Lie-algebra fields" for the integration. In this sense, neither of the two methods uses the projection into SU(3) for the flowed or smeared link variables.

The gradient flow equation can be regarded as a continuous version of the link fuzzing step in the stout smearing as pointed out in the original paper [3]. Moreover, the authors of Ref. [4] relate the smoothing parameter for other smoothing schemes to the gradient flow time τ under the assumption that the lattice spacing and the smearing parameter are small enough. For the case of

the stout smearing, the corresponding flow time τ is given by the matching relation of $\tau = \rho \times n_{\rm st}$ with the number of stout smearing steps $n_{\rm st}$ for the isotropic four-dimensional case of the smearing parameters ($\rho_{\mu\nu} = \rho$).

In Fig. 3, we show the effective masses of the 0^{++} glueball state obtained from the spatial gradient flow and the stout smearing at the same flow time τ that is determined by the matching relation between the two methods. In this work, for the stout smearing, the spatially isotropic three-dimensional parameter set is chosen to be $\rho_{ij} = \rho = 0.1$ and $\rho_{4\mu} = \rho_{\mu 4} = 0$. The numerical correspondence between the two methods is clearly observed in both the lower and higher diffusion cases as shown in Fig. 3. It is worth remarking that the values of $n_{\rm st}$ adopted in Fig. 3, is much larger than a typical value of less than 10 in the usual usage. Although the usage of the stout smearing with a small value of $n_{\rm st}$ is not effective for the glueball calculations, the almost identical result to the one made by the spatial gradient flow with the diffusion radius ($\sqrt{6\tau}$) can be obtained by the same amount of the diffusion radius ($\sqrt{6\rho n_{\rm st}}$) in the stout smearing.

Finally, we remark that both the spatial gradient flow and stout smearing methods share the strong isotropic nature in the extended glueball operators . We adopt five types of Wilson loop shapes (plaquette, rectangle, bent rectangle, fish, hand) [8] to construct the 0^{++} glueball operator. The shape-dependence of the resulting two-point functions disappears due to the strong isotropic nature after the large flow time or the high diffusion case. Therefore, the variational analysis [9, 10] based on the different shapes is not applicable. Instead of the different shapes, we can use the different diffuseness of the extended operator, which is given at the different flow time or the different smearing step, to carry out the variational analysis.

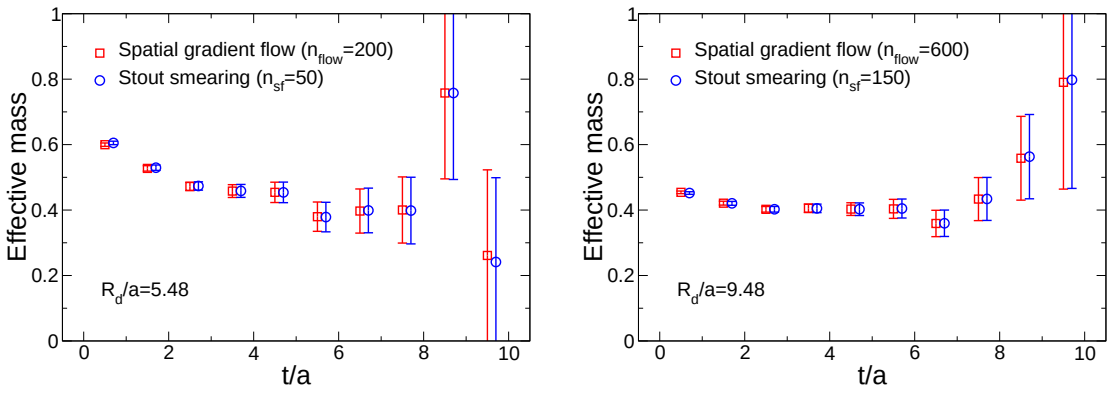

Figure 3: Comparisons of the effective mass plots using the spatial gradient flow and the stout smearing. The left panel is for the lower diffusion case ($\mathcal{R}_d/a = 5.48$), while the right panel is for the higher diffusion case ($\mathcal{R}_d/a = 9.48$).

3.4 Comparison with previous results for the 0^{++} glueball mass

Finally, It is worth comparing our result obtained from the spatial gradient flow with previous results obtained from the original gradient flow [5] (denoted as CHJ) and a conventional smearing [11] (denoted as AT). We calculate the glueball mass spectrum at four different lattice spacings

with a fixed physical volume $(1.6\ \mathrm{fm})^4$ as summarized in Table 1. In Fig. 4, we show our results of the 0^{++} glueball mass calculated by the spatial gradient flow method for a comparison with previous works. Our two data points obtained at the coarser lattice spacings are in good agreement with both CHJ and AT results, while the other two data points calculated at the finer lattice spacings are consistent with the continuum result of AT.

A more detailed comparison of the AT results computed with high precision reveals that our results are slightly overestimated. This is simply due to the effect of residual excited states contamination that is still in our analysis. We evaluate the 0^{++} glueball mass by a single exponential fit on the glueball two-point function computed at a fixed flow time, though the AT results are obtained through the variational analysis. We have indeed confirmed that the results given by the variational analysis, where the transfer matrix is constructed with the extended operators computed at different flow times, are slightly shifted closer to the AT results.

We next would like to assess effectiveness of our proposed method in comparison to the conventional approaches. A simple indicator of effectiveness or efficiency of a given method to calculate the glueball mass is defined as the following index:

$$\text{Effectiveness index (EI)} = \left[\frac{\text{(Error)}}{\text{(Central value)}}\right]^2 \times \text{(No. of measurements)}, \tag{6}$$

which corresponds to the relative size of the square of the signal-to-noise ratio with respect to the statistics. Table 2 compiles the values of effectiveness of respective smearing methods among three simulations (CHJ, AT and this work) performed at the similar lattice spacing ($\beta \approx 6.4$). According to the EI value, the spatial gradient flow or the stout smearing with the high value of n_{st} is several times more effective than the original gradient flow and the conventional smearing method.

It should be noted that the EI value does not reflect actual efficiency since the computational cost for the gradient flow method is relatively higher than the conventional smearing methods. Nevertheless, the above mentioned efficiency of the spatial gradient flow would have an advantage in dynamical lattice QCD simulations for glueball observables.

Table 2: Comparison of effectiveness of respective smearing methods among three simulations (CHJ, AT and this work) performed at the similar lattice spacing ($\beta \approx 6.4$). N_{total} denotes the number of total measurements in each simulation.

label	β	$L^3 \times T$	N_{total}	method	$aM_{0^{++}}$	EI
This work	6.40	$32^3 \times 32$	3000	Spatial gradient flow	0.404(9)	1.5
				Stout smearing (high n_{st})	0.403(9)	1.5
				Stout smearing (low n_{st})	0.442(31)	14.8
				Gradient flow ($R_d = 0.23$ fm)	0.446(14)	3.0
CHJ [5]	6.42	$32^3 \times 64$	1958	Gradient flow ($R_d = 0.3$ fm)	0.393(15)	2.9
				Gradient flow ($R_d = 0.35$ fm)	0.387(18)	4.2
AT [11]	6.338	$30^3 \times 30$	80000	Conventional smearing [12]	0.4276(37)	6.0

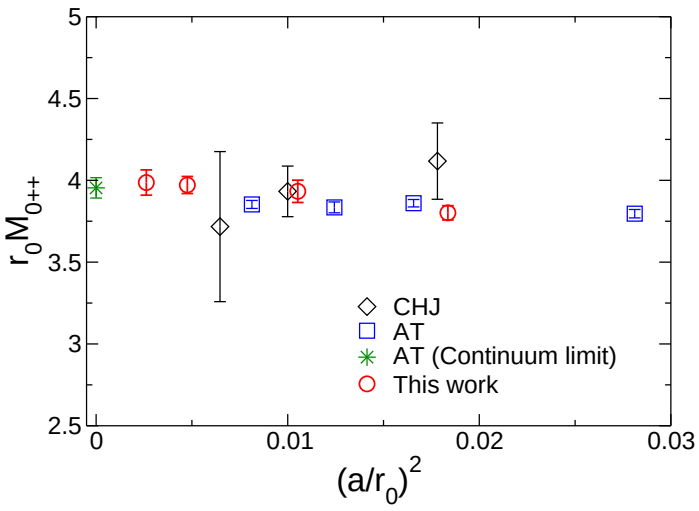

Figure 4: Comparison with previous results of the 0^{++} glueball mass. Our results are calculated by the spatial gradient flow method, while the CHJ and AT results are given by the ordinary gradient flow and the conventional smearing, respectively.

4. Summary

We have studied the glueball two-point function with two types of the gradient flow method. The original gradient flow, which makes the Wilson flow diffused in the four-dimensional space-time, has some problem in measuring the glueball mass from the two-point function. It is known to be *over smearing* due to the overlap of two glueball operators extended in both space-time as reported in the previous study [5]. This particular issue makes the plateau behavior uncertain in the effective mass plot, so that it is difficult to extract the ground-state mass of the glueball with high accuracy. To avoid over smearing, we propose the spatial gradient flow approach and also apply it to the glueball calculation. Our numerical simulations show that the spatial gradient flow method works well as a noise reduction technique, meanwhile it has a good property that the plateau behavior in the effective mass plot does not change with variation in flow time for sufficiently large flow time. The latter gives an advantage for extracting the ground-state mass of the glueball with high accuracy without over smearing. We have also showed numerical equivalence between the spatial gradient flow and the stout smearing in the glueball calculations from the low diffusion case to the high diffusion case. It means that the extracted glueball mass with the spatial gradient flow is surely the universal result that does not depend on details of the smearing procedure. Furthermore, to assess effectiveness of our proposed method, we have compared to the previous results of the 0^{++} glueball mass. We found that the spatial flow is a few times more effective than the original gradient flow and the conventional smearing method. Indeed, the precision of our results are comparable to that of the AT results, though our results are obtained with much smaller number of measurements than the AT results[11].

Acknowledgments

Numerical calculations in this work were partially performed using Yukawa-21 at the Yukawa Institute Computer Facility, and also using Cygnus at Center for Computational Sciences (CCS), University of Tsukuba under Multidisciplinary Cooperative Research Program of CCS (MCRP-2021-54). This work was supported by Graduate Program on Physics for the Universe (GP-PU).

References

[1] M. Albanese *et al.* [APE], Phys. Lett. B **192**, 163-169 (1987).

[2] C. Morningstar and M. J. Peardon, Phys. Rev. D **69**, 054501 (2004).

[3] M. Lüscher, JHEP **08**, 071 (2010) [erratum: JHEP **03**, 092 (2014)].

[4] C. Alexandrou, A. Athenodorou, K. Cichy, A. Dromard, E. Garcia-Ramos, K. Jansen, U. Wenger and F. Zimmermann, Eur. Phys. J. C **80**, 424 (2020).

[5] A. Chowdhury, A. Harindranath and J. Maiti, JHEP **02**, 134 (2016).

[6] R. Sommer, Nucl. Phys. B **411**, 839-854 (1994).

[7] S. Necco and R. Sommer, Nucl. Phys. B **622**, 328-346 (2002).

[8] C. Michael and M. Teper, Nucl. Phys. B **314**, 347-362 (1989).

[9] C. Michael, Nucl. Phys. B **259**, 58-76 (1985).

[10] M. Lüscher and U. Wolff, Nucl. Phys. B **339**, 222-252 (1990).

[11] A. Athenodorou and M. Teper, JHEP **11**, 172 (2020).

[12] B. Lucini, M. Teper and U. Wenger, JHEP **06**, 012 (2004).